Electronic Supplementary Information

A New Redox Strategy for Low-Temperature Formation of Strong Basicity on Mesoporous Silica

Li Zhu, Feng Lu, Xiao-Dan Liu, Xiao-Qin Liu, and Lin-Bing Sun*

State Key Laboratory of Materials-Oriented Chemical Engineering, College of Chemistry and Chemical Engineering, Nanjing Tech University, Nanjing 210009, China.

*Corresponding author. E-mail: lbsun@njtech.edu.cn.

Experimental section

Materials synthesis.

Mesoporous silica SBA-15 was synthesized according to the procedure as follows.[1,2] In a typical synthesis, 2 g of triblock copolymer P123 ($EO_{20}PO_{70}EO_{20}$) was dissolved in 75 g of 1.6 M HCl aqueous solution with stirring at 40 °C. Then, 4.25 g of tetraethylorthosilicate (TEOS) was added to the homogeneous solution and stirred at this temperature for 24 h. Finally, the temperature was heated to 100 °C and held at this temperature for 24 h under static condition. The as-prepared sample was recovered by filtration, washed with water, and air dried at room temperature. For the removal of template, the as-prepared sample was treated in an air flow at 500 °C for 5 h with a heating rate of 2 $^{o}C\cdot min^{-1}$.

The base precursor, KNO_3, was introduced to the support SBA-15 by wet impregnation. An identical amount of KNO_3 (20 wt%) was used for the samples. Typically, 0.2 g KNO_3 was dissolved in 15 mL deionized water, followed by addition of 0.8 g SBA-15. After stirring at room temperature for 24 h, the mixture was evaporated at 80 °C and subsequently dried at 100 °C for 4 h. The obtained material was denoted as KS.

For the thermal conversion of base precursor KNO_3 to basic sites, the sample KS was heated to 400 or 600 °C in a nitrogen flow (20 $mL\cdot min^{-1}$) for 2 h; the resultant samples were denoted as KS-T400-2 and KS-T600-2, respectively. For the conversion of KNO_3 using the redox strategy, the sample KS was heated to 400 °C in a nitrogen flow (20 $mL\cdot min^{-1}$) containing the vapor of reducing agent (*i.e.* methanol). The methanol vapor was generated by bubbling liquid methanol with nitrogen at room temperature. The redox time (*n*) ranged from 0.5 to 2 h, producing the materials denoted as KS-R400-*n*.

Characterization.

X-ray diffraction (XRD) patterns of the materials were recorded using a Bruker D8 Advance diffractometer with monochromatic Cu Kα radiation in the 2θ range from 0.5° to 10° and 10° to 80° at 40 kV and 40 mA. Transmission electron microscopy (TEM) was captured to analyze the structural characterization of the materials on a JEM-2010 UHR electron microscope operated at 200 kV. The elemental distribution of materials was determined using energy dispersive X-ray spectroscopy (EDX). EDX was performed using a Hitachi S4800 in the scanning electron (SE) mode and the accelerating voltage was 20 kV. N_2 adsorption-desorption isotherms were measured using ASAP 2020 at –196 °C. The temperature selected to perform the degasification step was 150 °C, and the degasification time was 4 h. The Brunauer-Emmett-Teller (BET) surface area was calculated using adsorption data in a relative pressure ranging from 0.04 to 0.20. The total pore volume was determined from the amount adsorbed at a relative pressure of about 0.99. The pore size distribution of the mesoporous materials was calculated from the adsorption branch by using the Barrett–Joyner–Halenda (BJH) method. In order to characterize the conversion of KNO_3, Fourier transform infrared (IR) spectra of the samples diluted with KBr were carried out on a Nicolet Nexus 470 spectrometer with a spectra resolution of 2 cm^{-1}. Mass spectrometer (MS, HIDEN HAL201)-monitored temperature programmed decomposition was employed to examine the conversion of supported KNO_3. About 50 mg of sample was heated from the room temperature to 700 °C in a flow of He (20 $mL \cdot min^{-1}$), and gaseous products derived from KNO_3 decomposition was analyzed by MS. For the conversion of KNO_3 using the redox strategy, the methanol vapor was generated by bubbling liquid methanol with He at room temperature. In situ IR spectra were recorded on an Agilent Cary 660 FTIR Spectrometer equipped with MCT detector (128 scans at a spectral resolution of 2 cm^{-1}) with a homemade in situ transmission cell. A vacuum level of < 0.01 mTorr in the transmission cell can be reached through a vacuum manifold, which is connected to a mechanical pump and a diffusion pump. A small amount of KS sample was loaded to a custom-made sample holder, followed by annealing at 200 °C for 4 h under vacuum to completely remove adsorbed water. After heating up to 400 °C, methanol was introduced to the transmission cell, and IR spectra were collected every 20 min in the process.

To measure the amount of basic sites, the samples (50 mg) after activation was added to aqueous HCl (0.05 M, 10 mL). The resulting suspension was shaken for 24 h and the slurry was separated by a centrifuge. The remained acid in liquid phase was titrated with standard base (0.01 M aqueous NaOH) and phenolphthalein was employed as an indicator. The amount of HCl consumed was used to calculate the amount of basic sites. Temperature programmed desorption of CO_2 (CO_2-TPD) experiments were conducted on a BELSORP BEL-CAT-A apparatus. The sample was activated at 400 °C (or 600 °C) for 2 h prior to the adsorption of

CO_2 (99.999%) at room temperature. After the physical adsorbed CO_2 was purged by a He flow (99.999%) at room temperature, the sample was heated to 800 °C at the rate of 8 °C·min^{-1}, and the CO_2 liberated was detected by MS.

Catalytic test.

The obtained basic materials were employed to catalyze the synthesis of dimethyl carbonate (DMC) via the transesterification of ethylene carbonate and methanol.[3] In a typical process, methanol (0.5 mol), ethylene carbonate (0.1 mol), and catalyst (0.5 wt% of methanol) were added to a three-necked glass flask with a water-cooled condenser. The reaction was conducted at 65 °C with stirring for a given period of time. After the reaction was completed, the reaction mixtures were recovered from the flask and subjected to centrifuging. The obtained upper liquid was then analyzed by use of a Varian 3800 gas chromatography equipped with a flame ionization detector.

Additional results and discussion

In addition to methanol, ethanol and H_2 were also employed as reducing agents. IR spectra show that the vibration band at 1383 cm^{-1} assigned to nitrate decreased gradually with the increase of reduction time in the presence of either ethanol or H_2 (Fig. S15 and S16, ESI†). However, a certain amount of KNO_3 remained even after 2 h, which is different from what happened in the presence of methanol. The amount of basic sites of resultant materials was also measured and the results are summarized in Fig. S17 (ESI†). The amount of basic sites using different reducing agents decreases in the order of methanol > ethanol > H_2. On the basis of these results, it is obvious that alcohols are better reducing agents as compared with H_2, and the alcohol with a small molecular size is superior to the large one.

Despite the fact that great efforts have been made, the construction of strong basicity on mesoporous silica through a facile method is still an open question to date. In the present study, we developed a redox strategy by using the oxidizability of nitrate precursors. The vapor of the reducing agent diffuses into the pores of support and interacts with predispersed KNO3. Because of the redox interaction, the conversion of the precursor to basic sites occurs at rather low temperatures, which breaks the tradition of thermally induced decomposition that usually requires much high temperatures. The reactions of strongly basic species with siliceous supports that occur at elevated temperatures can thus be avoided. As a consequence, materials possessing both ordered mesostructure and strong basicity were successfully constructed, which are highly expected for catalysis and improbable to achieve by conventional methods. In contrast to the traditional methods for the fabrication of mesoporous solid bases (e.g. basic group immobilization and nitrogen incorporation), our strategy offers a facile, efficient, and energy-saving method to create much stronger basicity on mesoporous silica. Such a strategy may open up an avenue to the design and synthesis of new functional materials.

References

1 D. Y. Zhao, J. L. Feng, Q. S. Huo, N. Melosh, G. H. Fredrickson, B. F. Chmelka, G. D. Stucky, *Science*, 1998, **279**, 548.

2 J. Nakazawa, B. J. Smith and T. D. P. Stack, *J. Am. Chem. Soc.*, 2012, **134**, 2750.

3 X. Y. Liu, L. B. Sun, F. Lu, T. T. Li and X. Q. Liu, *J. Mater. Chem. A*, 2013, **1**, 1623.

4 L. B. Sun, X. Y. Liu, A. G. Li, X. D. Liu and X. Q. Liu, *Chem. Commun.*, 2014, **50**, 11192.

5 T. T. Li, L. B. Sun, X. Y. Liu, Y. H. Sun, X. L. Song and X. Q. Liu, *Chem. Commun.*, 2012, **48**, 6423.

6 X. Y. Liu, L. B. Sun, F. Lu, X. D. Liu and X. Q. Liu, *Chem. Commun.*, 2013, **49**, 8087.

7 X. Y. Liu, L. B. Sun, X. D. Liu, A. G. Li, F. Lu and X. Q. Liu, *ACS Appl. Mater. Interfaces*, 2013, **5**, 9823.

Table S1. The yield of DMC under the catalysis of various solid bases.[a]

Catalyst	DMC yield (%)				Ref.
	0.5 h	1 h	2 h	4 h	
MgO	1.3	2.9	4.7	7.6	4
KL	1.0	2.5	3.0	4.0	5
CsX	3.0	4.5	5.2	6.1	6
Li_2O/Al_2O_3	12.5	14.6	17.8	18.8	4
Na_2O/Al_2O_3	18.0	22.5	25.1	28.2	7
CaO/ZrO_2	7.0	10.1	12.3	15.1	6
CaO/SBA-15	2.0	5.4	12.0	13.4	5
K_2O/C/SBA-15	26.4	30.6	34.5	38.6	7
K_2O/ZrO_2/SBA-15	11.9	19.4	24.9	28.4	3

[a] MgO was obtained by calcining the precursor $Mg(NO_3)_2{\cdot}6H_2O$ at 500 °C for 4 h. The zeolite KL was a commercially available catalyst. The zeolite CsX was prepared by ion exchange of NaX with $CsNO_3$ for 3 times. Li_2O/Al_2O_3 was obtained by impregnation of $LiNO_3$ into Al_2O_3 followed by calcination at 600 °C for 2 h. Na_2O/Al_2O_3 was prepared by impregnation of NaOH into Al_2O_3 followed by calcination at 600 °C for 2 h. CaO/ZrO_2 was obtained by impregnation of $Ca(NO_3)_2$ into ZrO_2 followed by calcination at 550 °C for 2 h. CaO/SBA-15 was prepared by impregnation of $Ca(NO_3)_2$ into SBA-15 followed by calcination at 550 °C for 2 h. K_2O/C/SBA-15 was obtained by impregnation of KNO_3 into the support C/SBA-15 followed by calcination at 400 °C in N_2 for 3 h; the support C/SBA-15 was produced by introducing furfuryl alcohol and oxalic acid to SBA-15 followed by polymerization and carbonization. K_2O/ZrO_2/SBA-15 was prepared by introducing KNO_3 to the support ZrO_2/SBA-15 followed by calcination at 550 °C in N_2 for 200 min. The support ZrO_2/SBA-15 was produced by precoating a layer of ZrO_2 on SBA-15.

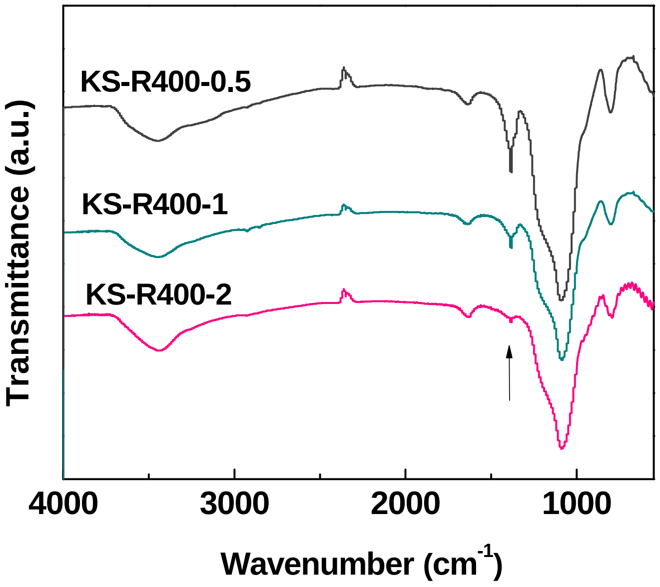

Fig. S1 IR spectra of KS treated by the redox strategy for different time (0.5, 1, and 2 h).

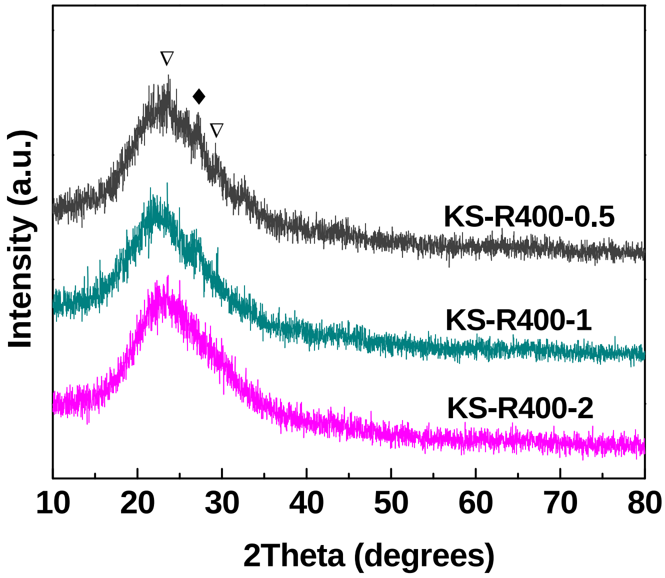

Fig. S2 Wide-angle XRD patterns of KS treated by the redox strategy for different time (0.5, 1, and 2 h). ▽and ◆ denote KNO_3 of orthorhombic and hexagonal phases, respectively.

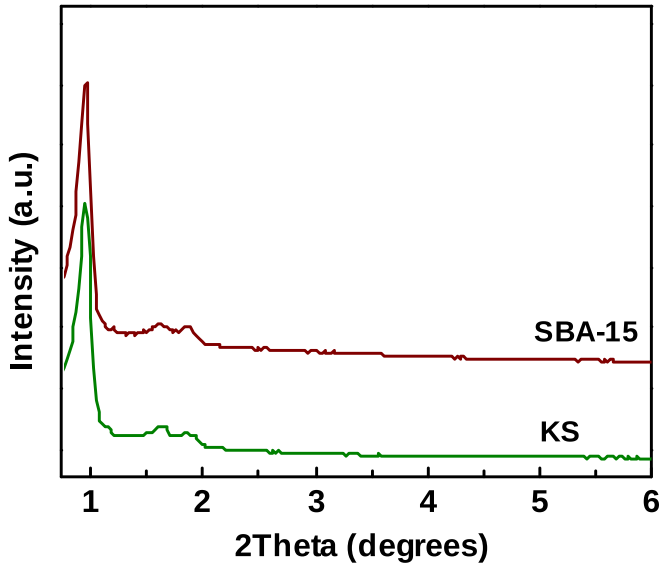

Fig. S3 Low-angle XRD patterns of the samples SBA-15 and KS.

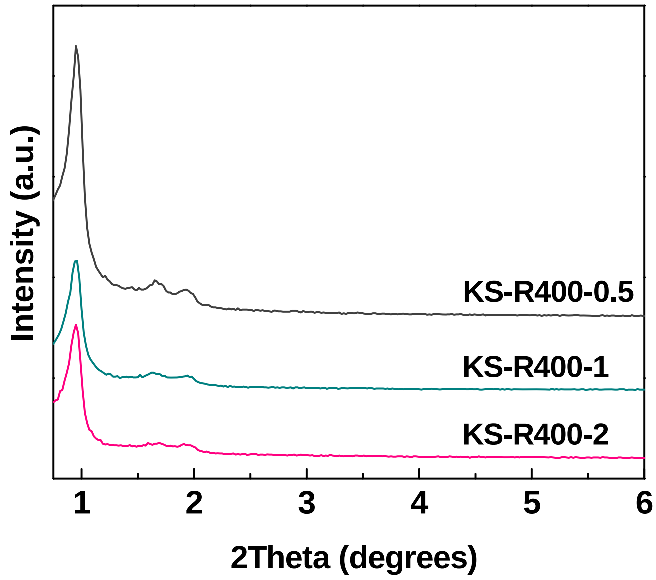

Fig. S4 Low-angle XRD patterns of KS treated by the redox strategy for different time (0.5, 1, and 2 h).

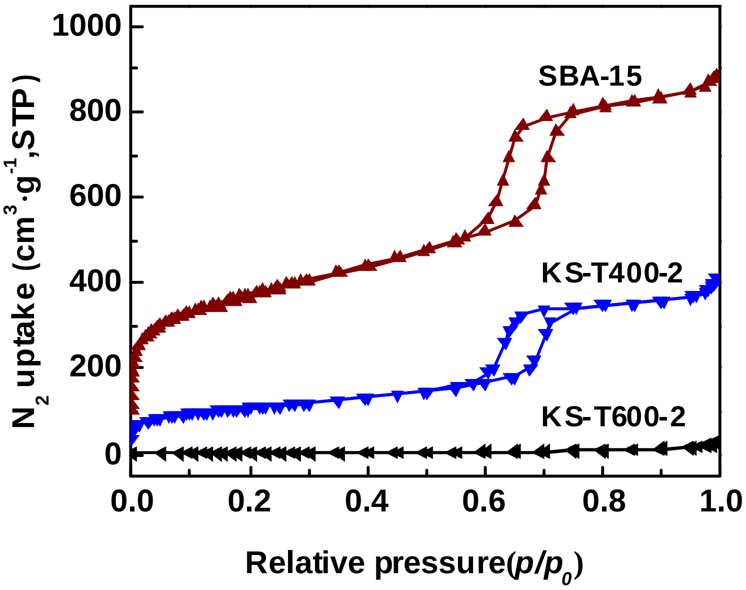

Fig. S5 N_2 adsorption-desorption isotherms of SBA-15, KS-T400-2, and KS-T600-2 samples. For clarity, curves of SBA-15 and KS-T400-2 are offset by 100 and 20 $cm^3 \cdot g^{-1}$, respectively.

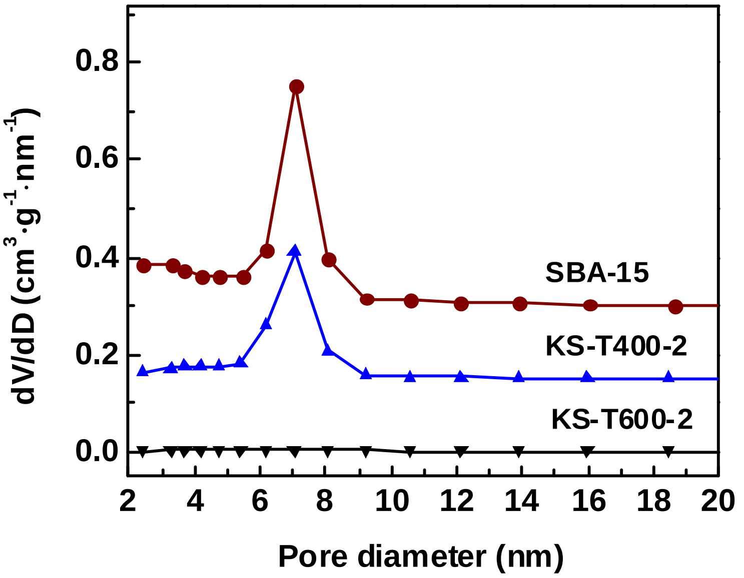

Fig. S6 Pore size distributions of SBA-15, KS-T400-2, and KS-T600-2 samples. For clarity, curves of SBA-15 and KS-T400-2 are offset by 0.30 and 0.15 $cm^3 \cdot g^{-1}$, respectively.

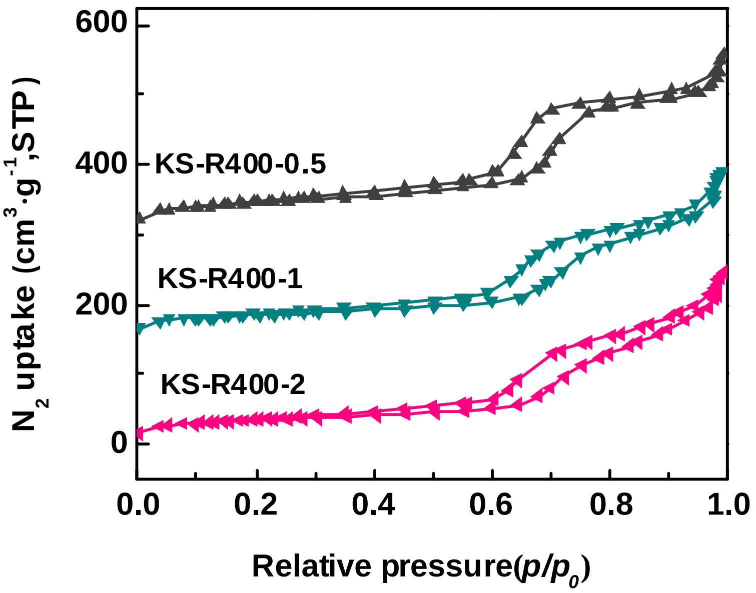

Fig. S7 N_2 adsorption-desorption isotherms of KS treated by the redox strategy for different time (0.5, 1, and 2 h). For clarity, curves of KS-R400-0.5 and KS-R400-1 are offset by 300 and 150 $cm^3 \cdot g^{-1}$, respectively.

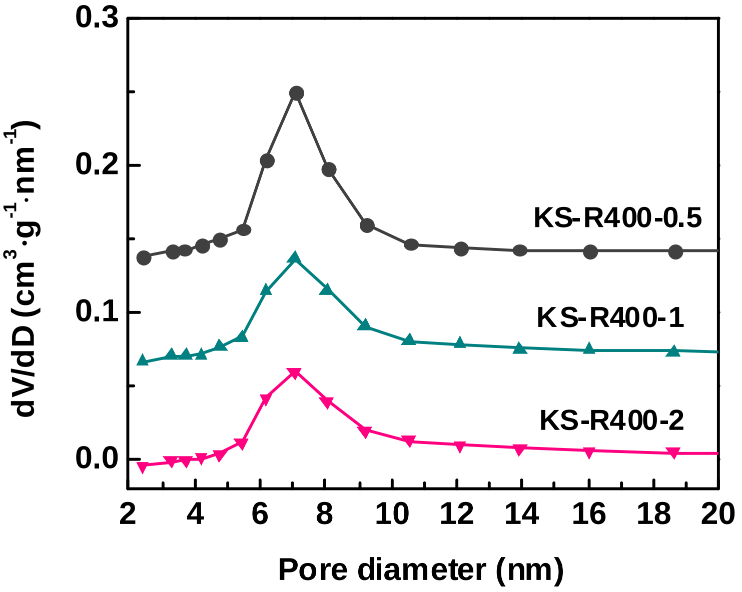

Fig. S8 Pore size distributions of KS treated by the redox strategy for different time (0.5, 1, and 2 h). For clarity, curves of KS-R400-0.5 and KS-R400-1 are offset by 0.14 and 0.07 $cm^3 \cdot g^{-1}$, respectively.

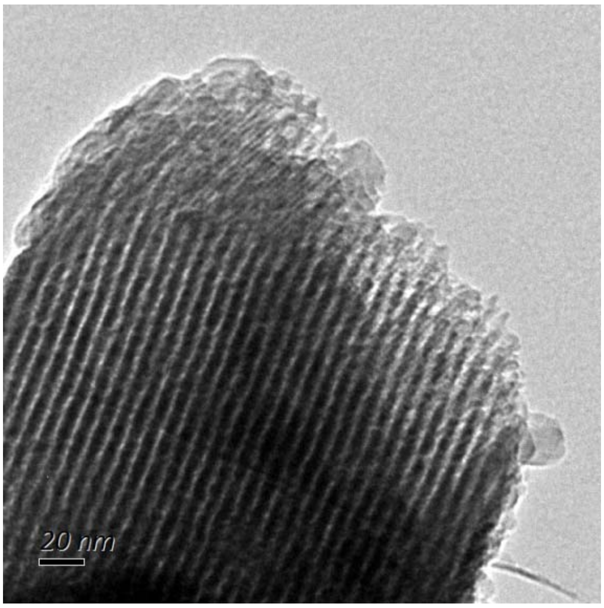

Fig S9 A TEM image of the sample KS-R400-2. The scale bar represents 20 nm.

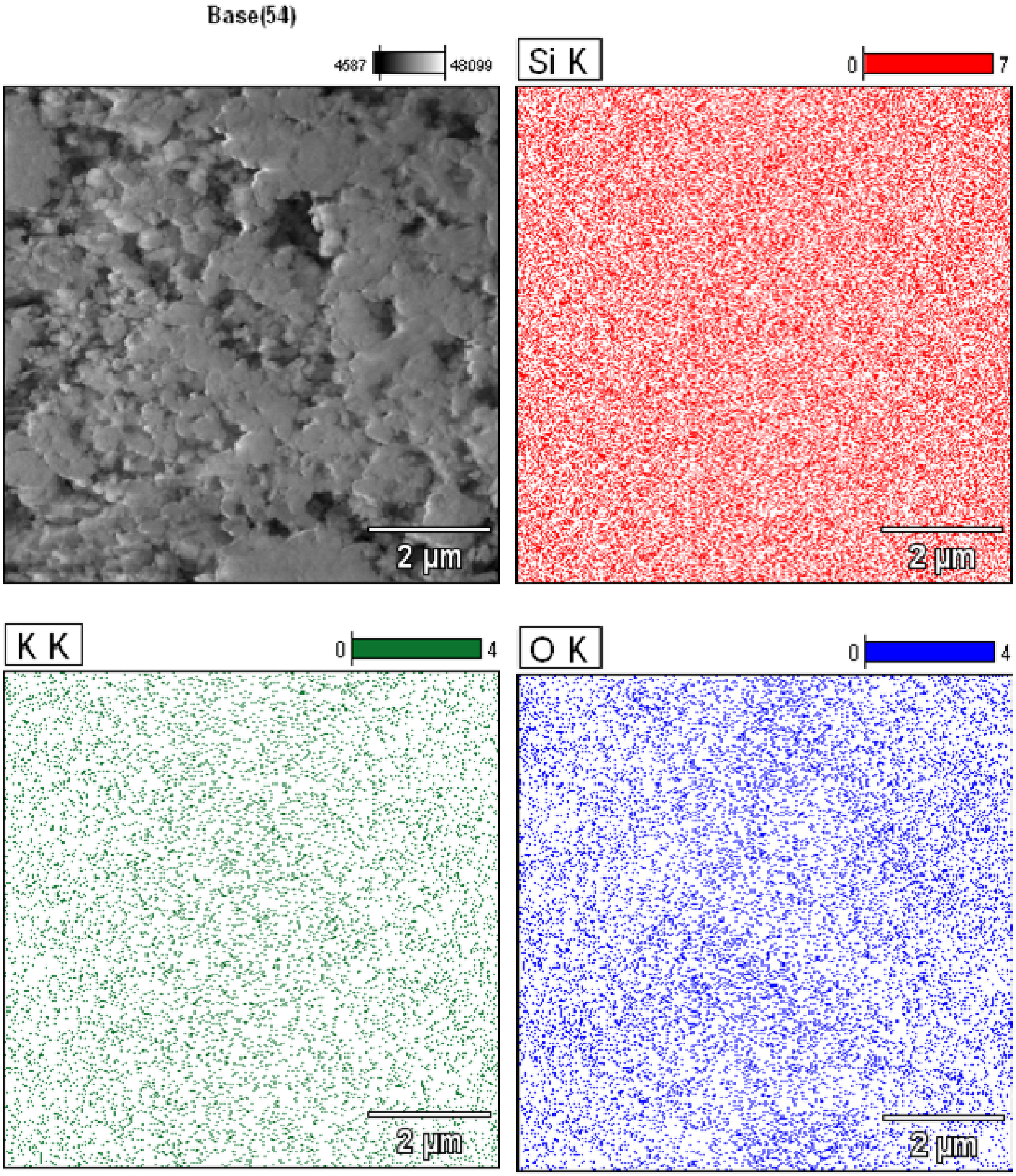

Fig. S10 EDX mapping of the sample KS-R400-2.

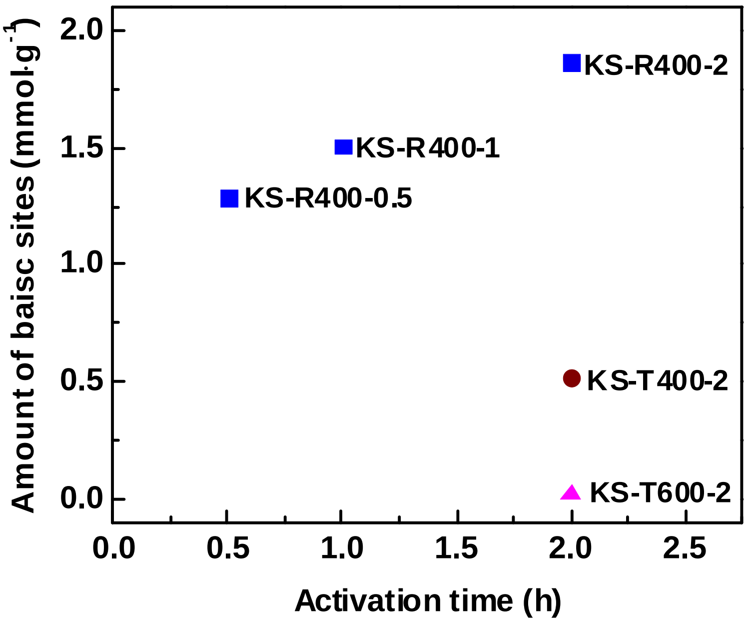

Fig. S11 Amount of basic sites of samples obtained through the conventional thermal method (at different temperatures) as well as the redox strategy (for different time).

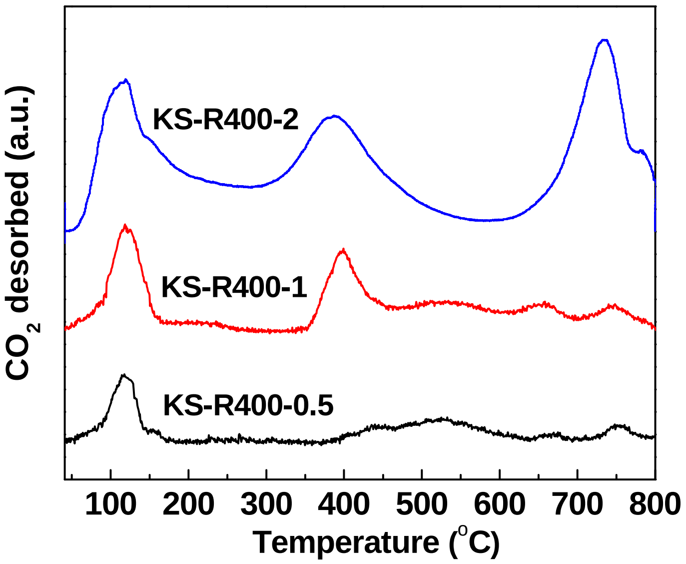

Fig. S12 CO_2-TPD profiles of KS-R400-0.5, KS-R400-1, and KS-R400-2.

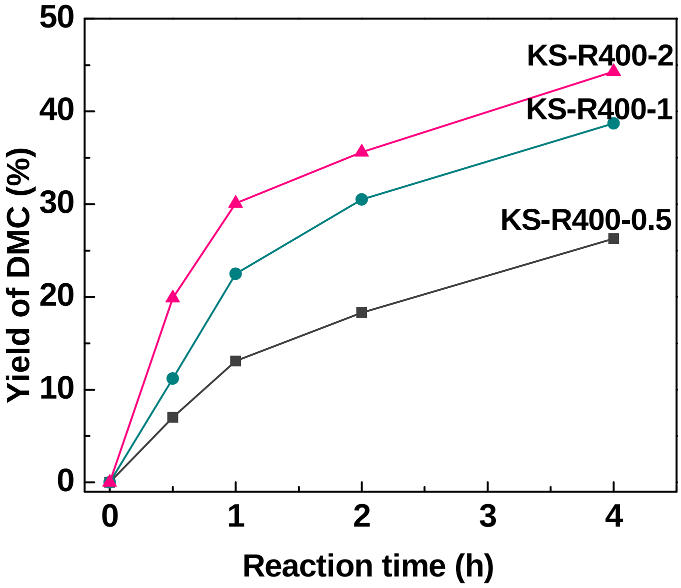

Fig. S13 The yield of DMC under the catalysis of KS treated by the redox strategy for different time (0.5, 1, and 2 h).

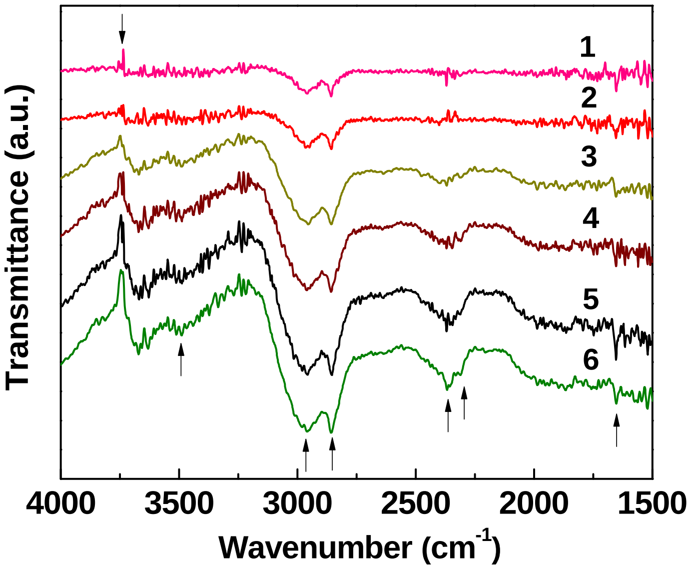

Fig. S14 In situ IR spectra of KS treated in MeOH at 400 °C.

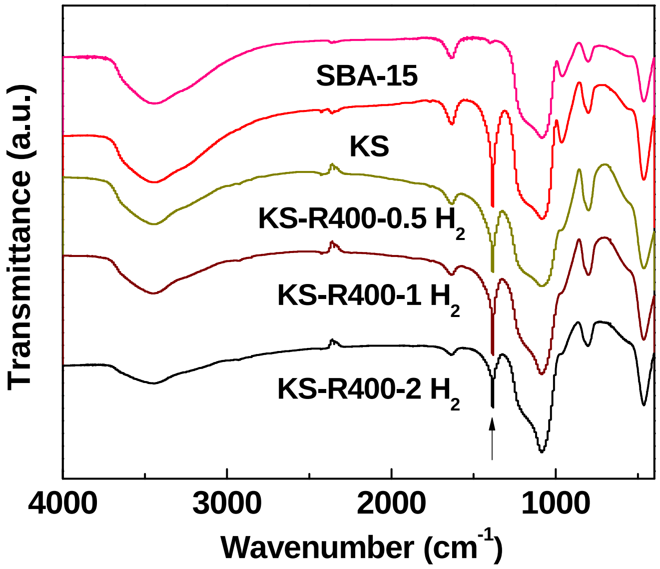

Fig. S15 IR spectra of KS treated in H_2 at 400 °C.

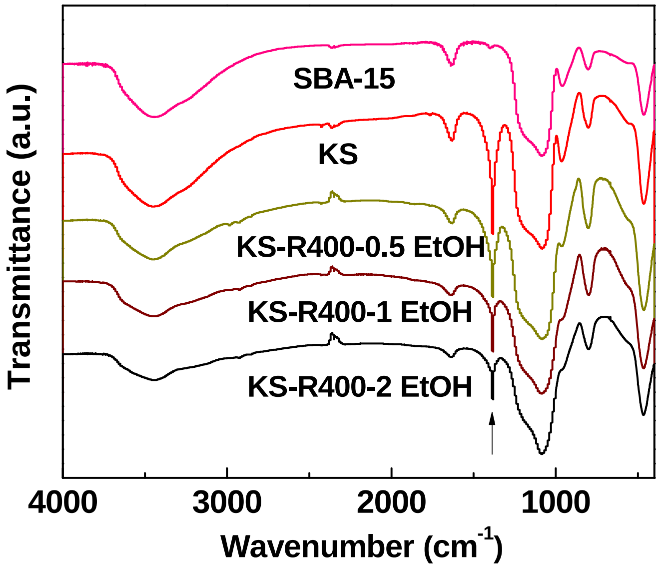

Fig. S16 IR spectra of KS treated in EtOH at 400 °C.

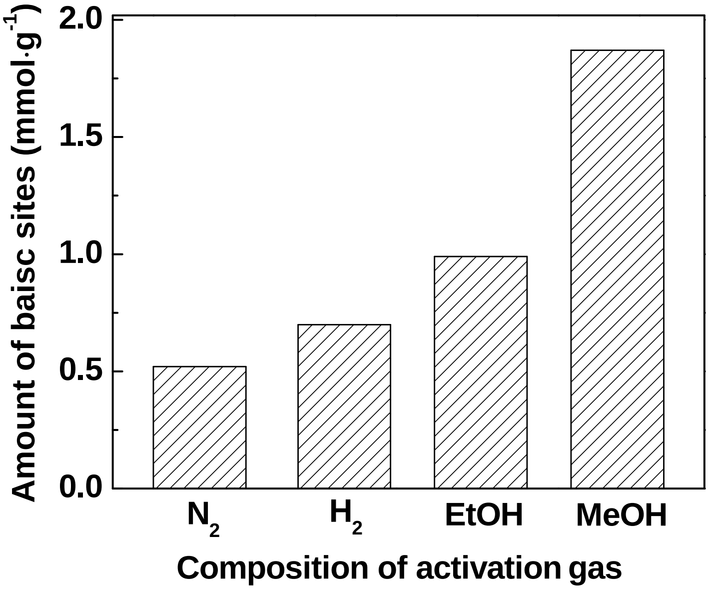

Fig. S17 Amount of basic sites of samples treated at 400 °C for 2 h in different activation gases.